[1]Y. Dhayaneswaran
A. Amudha[2]

Analysis and Measurement of Supraharmonics in Real Textile Industries Using Hybrid Technique

Journal of Electrical Systems

Abstract: - In this paper proposes a hybrid ADKF-FHO method for analysis and study of supraharmonics in textile industry. The proposed hybrid approach is the combined performance of anisotropic diffusion Kuwahara filtering (ADKF)and Fire Hawk Optimizer (FHO). Commonly it is named as ADKF-FHO technique. The major objective of the proposed approach is the main aim is to analysis of Supraharmonicsin real textile industries. The Variable frequency drive is predominantly used in Textile industry for varying the speed to control the roller speed for obtaining quality of yarn from the machine with more productivity and high energy saving. The ADLF is utilized to ensure the supraharmonics in textile industry and the FHO is used to optimizing the switching states of the embedded power converter. In this paper, standards and its limits are discussed; simulation model of the drive is done to ensure the Supraharmonics. Real time testing of the motor with drive for ensuring the Supraharmonics at testing laboratory and real time Textile industry in different geographical location is discussed in detail. By then, the proposed model is implemented in MATLAB/Simulink working stage and the execution is calculated with the existing methods. The proposed method shows better results in all approaches like RFA, CSA and PSO.

Keywords: *Harmonics, Electromagnetic Interference, Mitigation, Harmonic Frequency, Motor, Supraharmonics.*

I. INTRODUCTION

In Textile industry, power electronic devices of variable frequency drives, switched mode power supply, Un-interrupted power supply and Servo drives are in increasing trend due to fully automated machines [1]. But each of this type of new technologies causes problems for the electrical grids because they emit waves in the 0–2 kHz range. Also, in current history, the switching frequencies of converters using power electronics have been going to make equipment smaller and more efficient [2]. As a result, emissions in a new spectrum range of 2–150 kHz are named Supraharmonics, are starting to show up. The most important parts among those technologies are power converters, which include VFD, rectifiers, converters of DC to DC and inverters [3]. When they are added to electrical grid connections, they cause big problems with power quality, especially with Supraharmanic emissions [4].

Reason for more automation in textile industry is shortage of manpower due to dust and more noise inside the textile industry [5]. As the Textile industry runs continuously without any stoppage, maintaining the power electronic devices in healthy condition is at most important for the technicians [6]. If any of the devices fail, there will be huge profit loss [7].

Hence, the technician must be done all the preventive action from the power quality issues to avoid the failure or malfunction of the components [8].Recently, many problems like as household equipment failures, capacitoroverheating, and electromagnetic incompatibility have been reported due to strong SH emission. As a result of increased thermal stress induced by SH emissions, the life of electrical appliances is reduced [9]. The primary goal of the cotton mill is to make thread (yarn) out of raw cotton, which takes six steps to do [10]. The details of the processes are talked about briefly so that people who read can understand [11]. The cotton mill has a Blow room machine which cleans the raw cotton by removing un-wanted particles and fed the cleaned cotton into the Carding machine to form the cotton in to thick sliver (thick thread) by removing waste materials [12].

The output of the Carding machine (thick sliver) will further process with Draw frame and a comber machine. The comber machine gets rid of any short fibers that aren't wanted [13]. The uniform thickness of Sliver is fed

[1 1*]Research Scholar, Department of Electrical and Electronics Engineering, Karpagam Academy of Higher Education, Coimbatore, Tamil Nadu, India

[2]Professor, Department of Electrical and Electronics Engineering, Karpagam Academy of Higher Education, Coimbatore, Tamil Nadu, India

[*]Corresponding Author Email: dhayaneswaran.y@gmail.com

into Speed frame to make the Sliver in to Roving (thin sliver)[14]. Ring frame machine, converts roving to thin yarn (thin thread). Ring frame is real production of the cotton mill and will transport in to Autoconer machine to form a yarn into sellable package with different weights. The packaged yarn will be sent to fabric making section to produce the wearable cloths [15].

While visiting various textile industries for conducting power quality study, it is observed that there are failures on variable frequency drives at random [16]. On examination of the failure drives, noted the failure of DC choke and capacitors. The DC choke and capacitors are connected after the rectifier to filter the ripple content [17]. This failure is hitting the production to the large extend. During the visit to site 4, the failure of the drive is occurred during power quality study, the same is discussed in detail [18]. Also, we noticed that the Solar panels are installed in most of the Textile industry to compensate the electricity bill [19]. The Solar power is converted into AC through Inverter and connected into the medium voltage panel. So, the combination of the Solar power through inverter and increasing in variable frequency drive contributes more power quality concern in the Textile industry [20].The rest of the paper is mentioned as below: Section 2 describes recent research work and their background. Section 3 clarifies heat transfer enhancement configuration of heat exchanger. Proposed Methodologies Based Supraharmonics in Textile industry is illustrated in Section 4. Section 5 explains Simulation of VFD Model to Analyze the Supraharmonics. Section 6 concludes the paper.

II. RECENT RESEARCH WORKS: A BRIEF REVIEW

Numerous researches have earlier presented in the literatures were depending on Supraharmonics harmonic reduction in electric power grid by using various methods and aspects. Some of them were mentioned here,

According to S.T. Alfalahi et al. [21], the power electronics technologies related to smart grids and renewable energy systems (RES) have attracted increasing interest in the electric power distribution system. Electric power from RES was converted, controlled, or transferred to the power networks using power electronic devices. However, the constant rise in switching frequencies brought on by these power electronics equipment had resulted in the appearance of novel emissions on frequency 2-150 kHz, outside the conventional range for PQ. The term "supraharmonics" refers to these emissions (SH). The PQ of electrical distribution systems were adversely impacted by these emissions, and also shorten their lifespan and efficiency. Studying waveforms with spectral components 150 kHz and evaluating them. The historical context, the expanding availability of high switching frequency static converters, and expansion of Power Line Communication have all been utilized by G. Carpinelli et al. [22]. The simultaneous presence of a large count of spectral components with contrasting requirements for time frame length in the region of low- and high- frequencies makes it difficult for researchers to analyze such waveforms. The major goal was to use a collaborative way of analysis depending on successful divide and conquer approach to enhance the performance of other methods. The other methods ensure the optimal trade-off among accuracy and computing requirements. The effects of voltage and load unbalance, and conductor crosstalk on SHs have been demonstrated by Slangen et al. [23] using measurements and mathematical models. For constant power loads, the effect of voltage imbalance was discovered to boost the emission of supraharmonics. The influence of conductor crosstalk was demonstrated by the introduction of 2 new terminology, induced primary and secondary emission. The device's self-emission rises as a result of the primary emission that was induced. On the other side, the produced secondary emission affects the propagation of the emission. It was demonstrated how conductor crosstalk, load unbalance, and voltage unbalance all had an effect on the addition of SH emission in neutral-conductor.

According to an Espn-research Delgado [24], the transmission of supra harmonics through MV and LV grids interferes with end-user equipment and elements for power delivery, causing things like deterioration capacitor, light flicker, audible-noise, termination cable, and disruption of electric vehicle (EV) charging. Guidelines make it easier to diagnose issues associated to SH be required because these incidents occur more frequently. Different interferences were caused by different SH distortion characteristics. Solar and wind energy technologies received a lot of attention lately on electric power distribution system was introduced by Amudha, et al. [25]. It was able to transfer energy as natural power sources into electric power using power electronics equipment. Electronics advancements have caused at identification of novel emissions that happen among frequencies 2 and 150 kHz that were earlier unknown. Supraharmonics was the name given to these emissions that may be found

all over the world.O Sefl, et al. [26] discussed the result of lesser supraharmonics on partial discharge activity on insulation system sample using specified spherical cavity defect. The repeating sinusoidal oscillations used to represent the supraharmonics were modeled after or recorded to reflect common trends in power converter-equipped moderate to high-voltage electric subgrids. The test-sample was based on the oscillation at one cycle per period and a basic waveform at 50 Hz, and a measurement of the associated partial discharge activity. In order to characterize the effect of low-voltage (LV) loads, Angela Z. Hameed et al. [27] have shown how to analyze SH propagation by using a stochastic methodology. The influence of reinforcement grid methods was examined using scenarios of a strong and weak grid

A. Background of the Research Work

Recent research work reveals that supraharmonics harmonic reduction in the electric power grid for textile industry is the most difficult endeavor. Adopting practical methods which are created with a proper approach is one of the primary issues facing the electric power grid. Businesses can implement all feasible strategies to considerably increase their energy efficiency by using a harmonic analyzer. Industries can replace their outdated equipment with newer models due to the early identification of harmonic voltage, minimizing the possibility of further damage or total equipment shutdown. A non-sinusoidal waveform's multiple frequencies, amplitudes, phases, and other components can all be measured using a harmonic analyzer. Integrators, an input device, and multipliers make up the majority of it. Electrical system harmonics are examined with a harmonic analyzer. Electrical voltages and currents known as harmonics can cause issues with the electrical system's ability to produce power. Equipment and machinery malfunction as a result of the high harmonic voltage. Different industrial textile sectors in India are concerned with harmonic distortion. The effects of harmonic distortion rely on the electrical power system's tolerance for them and the equipment's sensitivity to harmonic voltage. The facility's harmonic analyzer is the ideal tool for performing a thorough power quality analysis to identify the wave forms of the current and voltage on their respective frequency spectra. The probable source of harmonic voltage can be thoroughly analyzed with the aid of harmonic analyzers. The solution to these issues is optimal detecting with cutting-edge technologies. Few control approaches are offered in related works to reduce supraharmonics in the electric power grid; the aforementioned restrictions have driven this study endeavor.

III. CONFIGURATION OF GRID CONNECTED MOTOR IN INDUSTRIAL TEXTILE

The harmonic frequencies ranged from 0 to 2 kHz. SH is concerned about noise levels above 2 kHz, which are a problem with numerous current devices, particularly those powered by renewable energy [28]. Any disruption of current or voltage waveforms that occurs within the 2 to 150 kHz spectrum range is referred to be SH. Two driving forces produced by a link among inverter and grid drive a current. The mechanism consists of Grid, Inverter, Converter, Filter and motor. The grid is connected to the inverter and it is control by the proposed technique. The filter is to extract the power from the grid and converter is connected to the motor. The purpose of the proposed system is to control the roller speed. Outline of Grid connected to motor in Industrial textile is shown in Fig 1.

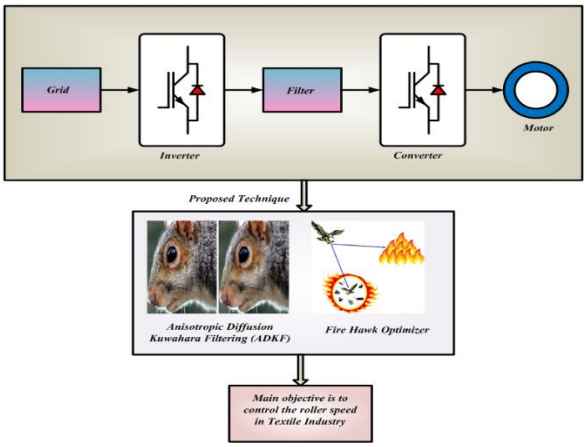

Fig 1: Outline of Grid connected to motor in Industrial textile

A. Single Tuned Passive Filter

Meanwhile, the fundamental frequency impedance of the filter should be high or the present load will not function properly. The goal is to avoid harmonic current that originates from the harmonic source by building the minimum impedance route at tuned frequency portrays on Fig 1. The filter's impedance can be determined by

$$z_f = r_f + J\left(x_{l_f} - x_{c_f}\right) \tag{1}$$

The frequency of tuned resonance F_{RES} of the provided STF to be allocated with power system on Hertz may be defined as:

$$F_{RES} = \frac{1}{2\pi\sqrt{l_f c_f}} \tag{2}$$

When the tuning frequency is reached, the inductive, capacitive, and reactance of filters cancels every one that provides:

$$H_{RES} = \sqrt{\frac{x_{c_f}}{x_{l_f}}} = \frac{F_{RES}}{F_{NOM}} \tag{3}$$

Where, H_{RES} refers tuning order, and F_{NOM} denotes nominal or fundamental frequency. The tuning resistor value r_f is provided as:

$$r_f = \frac{x_{cH}}{qf} \tag{4}$$

Where, $x_{cH} = \left(x_{l_f} * x_{c_f}\right)^{\frac{1}{2}}$ refers characteristics reactance and qf refers quality factor of tuning reactor [29-31].

B. Supraharmonics

In recent days numbers of variable frequency drives are in increasing trend in modern Industry including Textile Industry due to modernization of the plant, automation and energy saving on the machines resulting from such advancements in electronics field in high-power electronics has led to the appearance of novel emissions on frequency spectrum of two to one hundred fifty kilohertz. Supraharmonics are the collective name for such emissions. As the power electronics device population is high in the industry, maintaining the same in healthy condition is a real challenge to the end users. If any of the devices fails or malfunction, huge down time will cause profit loss. Hence, prevention of failure is in need now a day. The Harmonics mitigation is familiar in the industry, however Supraharmonics is not familiar [32].

Supraharmonics refers to any type of current or voltage waveform disturbance that occurs between the frequency ranges of 2 and 150 kHz. Several modern appliances, mainly those powered by renewable energy (RE), can cause concern for noise levels above 2 kHz. Supraharmonics are generated as electronic switching technologies split the sinusoidal voltage waveform among on and off states. Harmonics are named produced by circuits like inverter circuits. Electrical device failure, particularly touch screen technologies, mechanical resonant frequency noise, and thermal expansion stress are the entire probable outcomes of these enormous harmonics that may reduce equipment life. The most important sources of SH in the network are PLCs and power electronic converters. When dealing with constant loads, voltage quality affects current demand which, in

turn, affects the electrical grid. The variation of the voltage waveform causes a deviation of the current waveform [33].

Supraharmonics have the ability to be generated by main grid RE sources utilize inverters as output interfaces [34]. A current is driven through two driving forces produced with connection among inverter and grid, as shown in the figure below. A quantity of current created by power electronics or any other electrical equipment is conventional or supraharmonic in nature is called primary emission. Secondary emission is a constant or supraharmonic component of current created by sources outside to the device (e.g., power supply). The equivalent circuit for primary and secondary emission is shown in Fig. 2.

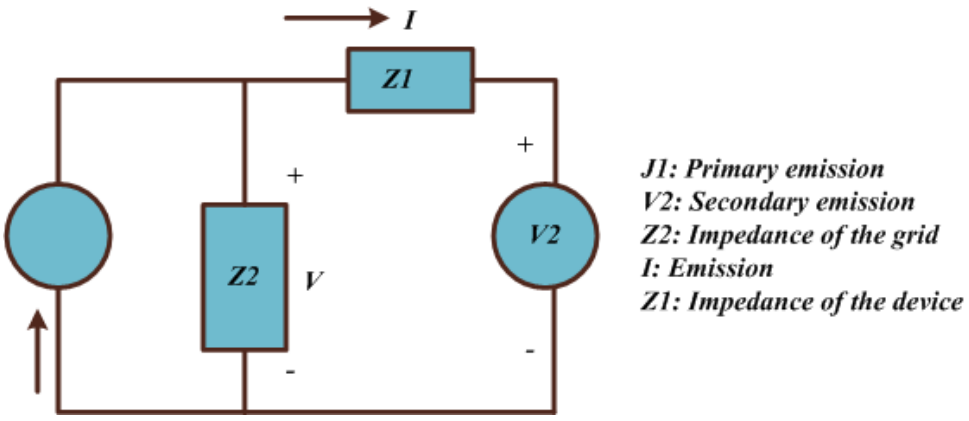

Fig 2: Equivalent circuit for emission of primary & secondary

Voltage and current are both important when it comes to Power Quality. Ohm's law states that voltage and current are connected via impedance Z. The voltages (URMS) and currents (IRMS) during charging, consists of individual harmonic currents (Ih) and voltages (Uh), supraharmonic components, and fundamental components (U1, I1) are of interest for each phase. The Fast Fourier Transform (FFT) can be used to calculate the harmonic and supraharmonic components. Additionally, total demand distortion is calculated using the maximal demand current (Imax) corresponding to the maximal charging power of the BEVs [35].

C. Textile Manufacturing Processes and Energy Profile

The five primary sub stages of the textile manufacturing process are fiber processing, spinning, weaving, wet processing, and garment manufacturing portrays on Fig.3 The first image depicts a typical woven textile product's general production path line. Figure's dotted boxes A and B represent the primary and secondary uses of energy in a typical textile production plant [36]. The primary energy-consuming production lines of spinning, sizing, and weaving are represented by the boxes 1, 2, and 3; process using water; and the production of clothing. Heating, cooling, sanitation, transportation, outdoor, and other energy-consuming applications are examples of secondary energy-consuming applications. Energy consumption varies depending on the manufacturing process. There are processes that use more energy than others. Each stage of the process requires a particular type of energy. Throughout the spinning process, electricity is used, which includes mix, open, preparation, spin, wind, and double [37].The quantity of energy required for this operation is influenced by the sort of spinning equipment, winding and doubling machinery, preferred yarn attributes, and raw material appearances. Spinning and winding techniques account for approximately 80% of the energy necessary per kilogram of single yarn under the case of middle count, carded, and ring yarn processing. Between the spinning and weaving processes, the sizing process is crucial. The majority of yarn sizing before warping requires indirect steam heated by electricity, gas, or oil. Electric energy is required for weaving processes. Measure of energy utilization is changes relying upon texture design and specialized boundaries of winding around machine [38].

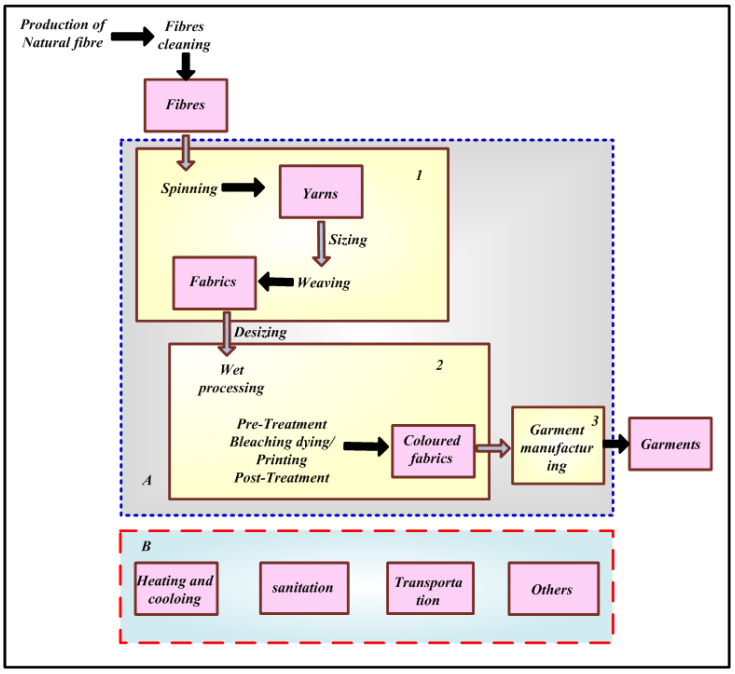

Fig 3: Textile flow process

The controlled climate of the spinning and weaving rooms, which have a temperature of 25 degrees Celsius and relative humidity of 65 percent, is another key electric energy-consuming station in the stages of textile manufacturing. The quantity of air conditioning systems that consume energy is also heavily influenced by seasonal fluctuations in weather [39]. Wet processing requires a substantial quantity of heat under the form of steam, hot air, and hot water throughout the pretreatment, bleaching, dyeing, post treatment, and drying-fixation stages. Electricity powers mechanical components of wet processing machinery. When compared to the other stages of textile processing, wet processing has relatively low total electric energy consumption. Clothing producing phases of resting up, cutting, sewing, cleaning with air pull, pressing, and shipping process generally consumes electric energy. Steam or hot air may be required for only heating ironing processes. Numerous industrial sectors are dissimilar, like the textile industry, are particularly interested in energy management research, improving energy efficiency, and possible energy savings [40-43]. Various industrial sectors have been the focus of numerous international and domestic projects aimed at energy management and energy efficiency enhancement. The P (plan), D (do), C (check), and A (action) cycles of the total quality management approach are used to describe energy management practices and methods. Boilers, steam systems, heat isolation, pneumatic leakage prevention, electric motors, and motion transmission systems are the most common energy-saving components found in industrial manufacturing facilities. Industrial manufacturing facilities should promptly implement accurate maintenance plans and procedures to avoid potential energy losses [44].

D. Standard for Industrial Application and Limits

Under this section, compatibility level for conducted disturbances is discussed with International standard [45-47]. Without any kind of standardization, the range of frequencies that falls under 2kHzto 150 kHz is called Supraharmonics. Nevertheless, since there are only a few standards that handle this frequency range, this statement is not entirely accurate. The number of standards which covers this spectrum is significantly lower compared to the number of standards that cover harmonics; nonetheless, it is possible because not only one but other national standards as well as military standards encompass this frequency range. Although the existence of standards describing harmonic limitations on general area of the network for low-order harmonics, it is crucial to highlight that standards covering the high-frequency range almost entirely specify measuring emissions in a laboratory under specific environmental circumstances. This contrasts with the situation with high-order harmonics, where there are no such restrictions. The IEC standards 61000 series include a variety of topics, some of which are nomenclature, explanations electromagnetic phenomena, assembly techniques, measuring methodologies and mitigating techniques [48].

IV. PROPOSED METHODOLOGIES BASED SUPRAHARMONICS IN TEXTILE INDUSTRY

In this paper proposed a hybrid technique for supraharmonies reduction in real textile industry. ADKF-FHO optimization solves the optimization problems over an incessant exploring space. The main objective of proposed optimization strategy is used to ensure the supraharmonics in textile industry. The detailed description is described as follows:

A. Anisotropic Diffusion Kalahari Filtering (ADKF)

Anisotropic diffusion(AD) is a nonlinear diffusion filtering method. Diffusion is a strategy for balancing noise variance and conserving boundary details in the absence of generating or losing substantial data content like edges, lines, or boundary features [49]. The adaptive smoothing technique known as nonlinear diffusion filtering is mostly focused on the local features of the data. The ADKF is used to reduce the dimensionality of data and minimizes the information loss.

When there are high-dominant edges, it reduces the diffusivity. An adaptive data blurring and boundary edge enhancement filtering method depends on work of Perona and Malik is called anisotropic diffusion filtering. Additionally, it reduces blurring to a minimum and addresses the linear distortion caused by localization constraints. The crisp edge over a data set among smooth regions is maintained by isotropic diffusion filtering, which is capable of significant smoothing. The data edges and boundary features are rarely over-sharpened by anisotropic diffusion filtering. In contrast to other filters, the proposed AD filtering method yields the best outcome for blurring undesirable data features, provides a diverse smoothening effect, and is simpler. Anisotropic diffusion results are fused with Krzysztof Bartyzel's adoptive Kuwahara filtering in the current study. As a result, adaptive Kuwahara filtering is used in this study to effectively maintain stable improved structure and directional characteristics, and the fusion process avoids harsh blurring and artifacts. The most effective method for researching medical data processing applications and a good pretreatment tool for segmentation is ADKF. The AD method is described by and makes use of the equilibration property of Fick's law.

$$h = d_t.\nabla u \tag{5}$$

Here ∇u denoted attentiveness gradient that causes flux h and preserves efficiently the gradient information on boundary. Relation among ∇u and h is linkedvia diffusion tensor d_t. Assume h and ∇u refers parallel, If not, it is referred to as anisotropic diffusion. The following is how the Fick's based continuity equation for the anisotropic diffusion approach is written:

$$\partial_t u = DICV\left(d_t.\nabla u\right) \tag{6}$$

The diffusion filtering offered by Malik is provided as,

$$\partial_t u = DIV\left(G\left|\nabla u\right|\right)^2 \nabla u \tag{7}$$

Diffusion may be exactly stated as,

$$G\left(s^2\right) = \frac{1}{1+S^2/\lambda^2} \text{ here } \lambda > 0 \tag{8}$$

Here g implies diffusivity that subsequent the flux function $\phi(S) = G\left(s^2\right)$restricts with $\phi'(S) \geq 0$ for $|s| \leq \lambda$ and $\phi'(s) < 0$ for $|s| \leq \lambda.\lambda$ performs critical role of contrast parameter as backward diffusion areas, and λ value must be higher than 0.

$$\partial_t u = \phi'(\nabla u) u_{nn} + G(|\nabla u|^2) u_{\xi\xi} \quad (9)$$

The output of AD filtering is applied to Kuwahara filtering to generate stable improved structure. The ADKF approach divides the filtering window into 4 sections, with mean values for every areas, $Mean_r$ and variance va_r^2 are designed with below calculation:

$$Mean_r = \frac{1}{p_r} \times \sum_{(X,Y)\in\theta_r} \varphi(F(X,Y)) \quad (10)$$

$$va_r^2 = \frac{1}{p_r} \times \sum_{(X,Y)\in\theta_r} \varphi(F(X,Y)) - Mean_r [(F(X,Y)) - Mean_r \varphi]^2 \quad (11)$$

Where, p_r refers number of pixels present onregion r, $F(X,Y)$refers input data function, φ denotes individual pixel and R ∈ {0, 1, 2, 3refersfilter window regions. Each separated area is looked at separately. Window size is improved by one in each cycle, and the mean and variance of data color intensity are computed with Formulae (10) and (11) each time a new window is opened. Finally, Kuwahara factors in the differences between 4 areas.

B. Fire Hawk Optimizer

A novel met heuristic algorithm known as FHO algorithm depends on foraging habits of brown falcons, black kites, and whistling kites [50]. By carrying flaming sticks on its beaks and talons, these Fire Hawks purposefully spread fire. FHO is used to optimizing the switching states of the embedded power converter. Fig 4 depicts the FHO schematic diagram.

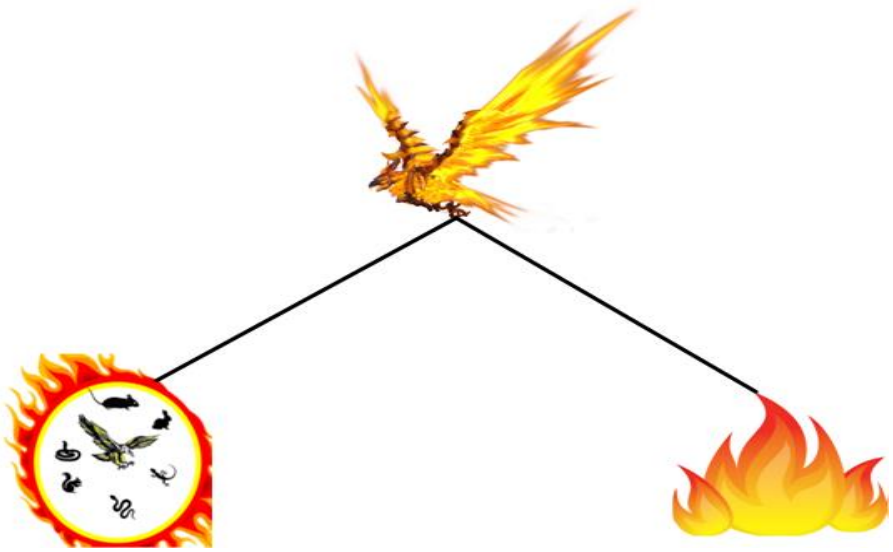

Fig 4: Schematic diagram of FHO

Fires that are purposely started or that develop naturally as a result of lightning can be spread by people and other sources. The specific behaviours that they do in nature to catch prey, including lighting it on fire, are the proposed FHO. To control and capture its prey, birds collect burning twigs and deposit them in other unburned areas to start minor fires. These little fires scare away prey, which includes mice, snakes, and other creatures, causing them to flee quickly and nervously, making it simpler for hawks to catch them. Flowchart of proposed FHO is depicted in Fig 5.

Step 1: Initialization

Initiate the input parameters such as voltage and current.

Step 2: Random Generation

After initiation, the input parameters are generated randomly in matrix form.

$$m = \begin{bmatrix} m_1 \\ m_2 \\ \vdots \\ m_u \\ \vdots \\ m_n \end{bmatrix} = \begin{bmatrix} m_1^1\ m_1^2 \cdots\ m_1^k \cdots\ m_1^d \\ m_2^1\ m_2^2 \cdots\ m_2^k \cdots\ m_2^d \\ \vdots\ \vdots\ \vdots\ \ddots\ \vdots \\ m_u^1\ m_u^2 \cdots\ m_u^k \cdots\ m_u^d \\ \vdots\ \vdots\ \vdots\ \ddots\ \vdots \\ m_n^1\ m_n^2 \cdots\ m_n^k \cdots\ m_n^d \end{bmatrix}, \begin{cases} u = 1, 2, \ldots, n. \\ k = 1, 2, \ldots, d. \end{cases} \tag{12}$$

Step 3: Fitness Evaluation

The fitness is evaluated depends on the objective function and it is defined as,

$$F = MIN(THD) \tag{13}$$

Step 4: Exploration Phase

$$M_u^k(0) = M_{u,MIN}^k + Rand.\left(M_{u,MAX}^k - M_{u,MIN}^k\right), \begin{cases} u = 1, 2, \ldots, n. \\ k = 1, 2, \ldots, d. \end{cases} \tag{14}$$

Where, M_u denoted as u^{th} solution candidate on search space; d denotes dimension; n refers total number solution candidates on search space; M_u^k refers k^{th} decision variable of u^{th} solution candidate; $M_u^k(0)$ denotes initial position of solution candidates; $M_{u,MIN}^k$ and $M_{u,MAX}^k$ refers minimal and maximal bounds of k^{th} decision variable of u^{th} solution candidate; and $Rand$ refers uniformly distributed random number on range of [0, 1].

Step 5: Determine the Global Best Solution

The objective function evaluation for the solution candidates evaluates the selected optimization problem in order to determine the placements of the Fire Hawks in the search space. Some solution candidates use higher objective function values portrayed as Fire Hawks, though the remainder is prey. Furthermore, the global best solution is supposed to be the main fire, which is initially used by the Fire Hawks to spread fires throughout the search space.

$$AB = \begin{bmatrix} AB_1 \\ AB_2 \\ \vdots \\ AB_i \\ \vdots \\ AB_j \end{bmatrix}, \ i = 1, 2, \ldots, j, \tag{15}$$

$$RS = \begin{bmatrix} RS_1 \\ RS_2 \\ \vdots \\ RS_f \\ \vdots \\ RS_g \end{bmatrix}, \ f = 1, 2, \ldots, g, \tag{16}$$

Where, AB_i refers i^{th} prey on search space with respect to total number of j prey and RS_1 is the j^{th} fire hawk contemplates the total number of g fire hawks on search space.

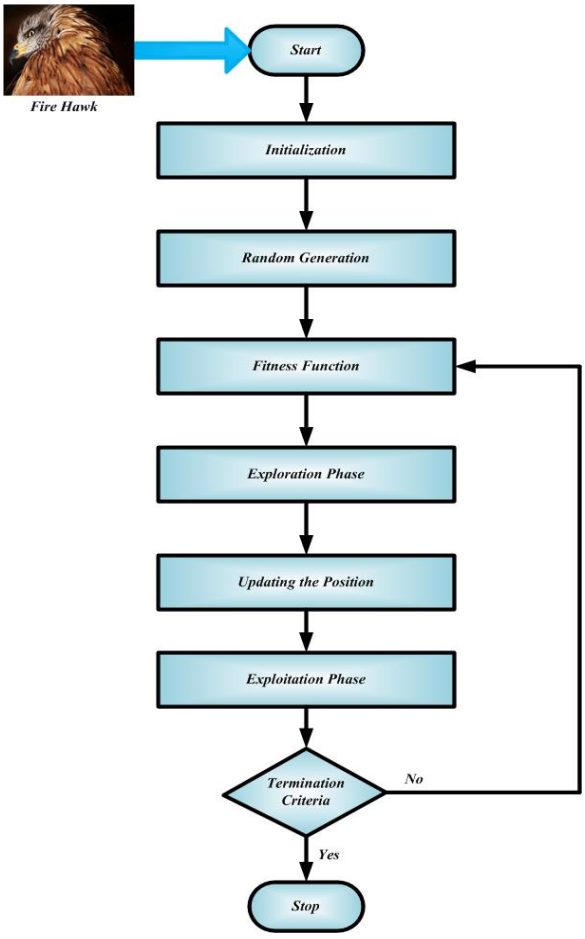

Fig 5: Flowchart of proposed FHO

Step 6: Compute Total Distance among Fire Hawks and the Preys

The overall distance among Fire Hawks and the prey is determined at following phase of the algorithm. The closest prey to every bird is identified, allowing these species' effective territories to be recognized. It should be renowned that the closest prey to the first Fire Hawk using best objective function value is determined, while the remaining prey is utilized to consider the territory of the other birds.

$$L_m^f = \sqrt{(w_2 - w_1)^2 + (z_2 - z_1)^2}, \ \begin{cases} f = 1, 2, \ldots, g \\ y = 1, 2, \ldots, j \end{cases} \tag{17}$$

Here, L_m^f refers total distance among f^{th} fire hawk and y^{th} prey; j refers total number of prey on search space; g refers total number of fire hawks on search space; $(w_1, z_1)$and (w_2, z_2) represent the coordinates of the Fire Hawks and prey in the search space.

Step 7: Determine the New Position of Fire Hawks

The fire hawks collect burning sticks from the main fire to establish fire in the designated area for position updating, the next stage of the algorithm. During this stage, each bird picks up a burning stick and drops it in its designated area, prompting the prey to run. In the meantime, certain birds are anxious to use burning sticks from other fire hawk territories; these two behaviours may be used as location updating methods on FHO's main search loop denotes below equation:

$$RS_1^{NEW} = RS_1 + (h_1 \times gb - h_2 \times RS_{near}), \quad f = 1, 2, \ldots, g, \tag{18}$$

Where, RS_1^{NEW} refers novel position vector of g^{th} fire hawk and gb defined as global best solution search space; h_1 and h_2 refers uniformly distributed random numbers on range (0, 1) determine the movements of fire hawks toward the main fire and other Fire Hawks territories.

Step 8: Compute the Safe Place in the Fire Hawks Territory

$$AB_q^{New} = AB_q + (h_3 \times RS_1 - h_4 \times VA_1), \begin{cases} f = 1, 2, \ldots, g \\ q = 1, 2, \ldots, h \end{cases} \tag{19}$$

Where, AB_q^{New} refers new position vector of q^{th} prey surrounded with f^{th} fire hawk and VA_1 implies safe place under f^{th} fire hawk territory.

Step 9: Calculate Safe Place outside the Fire Hawk's Territory

$$AB_q^{New} = AB_q + (h_5 \times RS_{alter} - h_6 \times VA), \begin{cases} f = 1, 2, \ldots, g \\ q = 1, 2, \ldots, h \end{cases} \tag{20}$$

Here, VA refers safe place outside of f^{th} fire hawk's territory and h_5 and h_6 refers uniformly distributed random numbers.

Step 10: Termination Criteria

Check the termination criteria and if the optimum outcome is obtained then the process is end else go to step 6.

V. SIMULATION OF VFD MODEL TO ANALYZE THE SUPRAHARMONICS

To confirm the Supraharmonics existence, The Variable frequency drive is predominantly used in Textile industry for varying the speed to control the roller speed for obtaining quality of yarn from the machine with more productivity and high energy saving. To confirm the Supraharmonics existence, VFD model is simulated through Matlab Simulink. Model is done with the Squirrel cage Induction motor with below mentioned parameters.

A. Supraharmonics Measurement on Variable Frequency Drive

Model file is done using with Matlab Simulink for 7.5kW drive; 7.5 kW drive. Matlab model with motor is portrays on Fig 6. Voltage wave form for the drive model is depicted in Fig 7. Here torque, voltage in and current in are considered. FFT analysis of the drive model for the voltage while motor is in load condition is

presented in Fig 8. As the simulation result is reveals that the Supraharmonics is present in the drive model, the same is to be confirmed in real time. To check the emission level of the Variable frequency drive in the band width between 2.0 kHz and 150 kHz, an Asynchronous induction motor of 7.5 kW is loaded through Variable frequency drive at its full capacity by varying the drive switching frequency from 2.5kHz to 8kHz. The data is captured through the PQ meter PQube-3that measures the Supraharmonics and the same is qualified for Class A conferring to IEC 61000-4-30 Ed3. Test setup to load the motor is portrays on Fig 9.The readings are taken from the meter while loading the motor its rated power in the test laboratory. The data is captured at the time of loading of the motor. Hence, the data is not captured in the graph during motor is not in running condition.Fig10. Depicts as, (a) One week data on Supraharmonics maximum peak voltage vs Frequency in kHz. (b) Trend of Phase to Earth graph for three phases from 2 kHz to 150 kHz (c) Phase to Earth graph 2 kHz to 150 kHz Conductive emission from PQ meter. The Maximum peak voltage is captured 30 volts at 4 kHz. The VFD trip issue noticed while observing the peak voltage. The graph shows the one-week maximum peak voltage vs Frequency 2 kHz to 150 kHz is plotted. Fig 11 depicts (a) Supraharmonics Peak Voltage vs Frequency (Weekly Data). (b) Phase to Earth Trends (2-150 kHz). (c) Conductive Emission Analysis (2-150 kHz). Maximum peak voltage is captured 14.5 volts at 2 kHz. The graph shows the one-week maximum peak voltage vs frequency spectrum from 2 to 150 kHz is plotted. Fig 12 shows (a) Supraharmonics Observation - Peak Voltage vs Frequency (Weekly). (b) Phase to Earth Trends (2-150 kHz). (c) Conductive Emission Analysis (2-150 kHz). Test set up near to the machine at Site 4 is depicted in Fig 13.The Maximum peak voltage is captured 65.8 volts at 2 kHz. The VFD trip and incoming fuse blown issue noticed while observing the peak voltage. The below graph shows the one-week maximum peak voltage vs Frequency 2 kHz to 150 kHz is plotted.

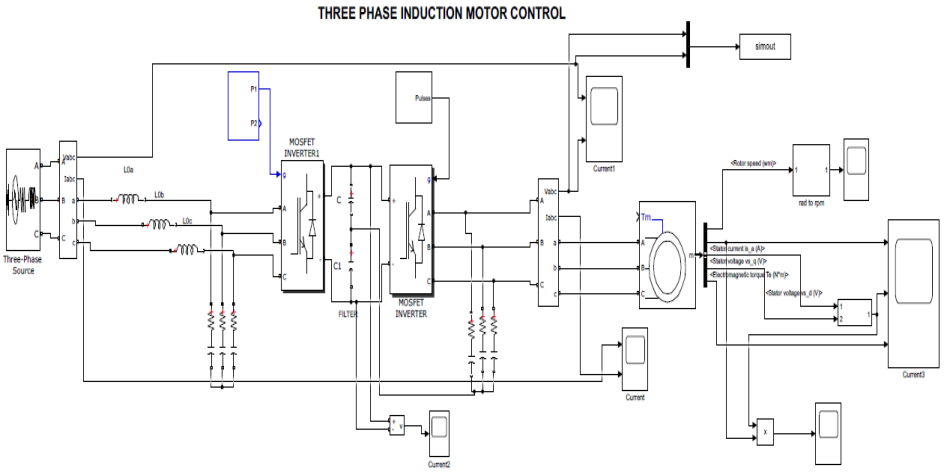

Fig 6: 7.5 kW drive Matlab model with motor.

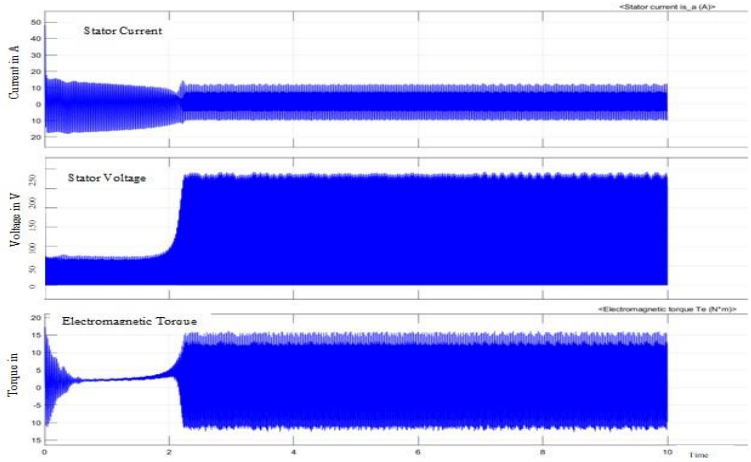

Fig 7: Voltage wave form for the drive model.

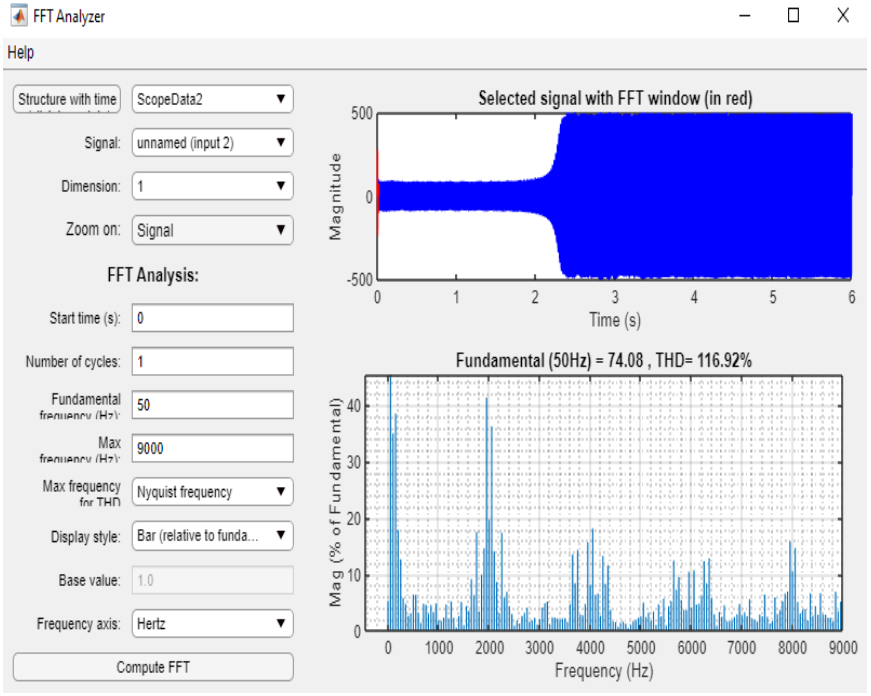

Fig 8: FFT analysis of the drive model for the voltage while motor is in load condition

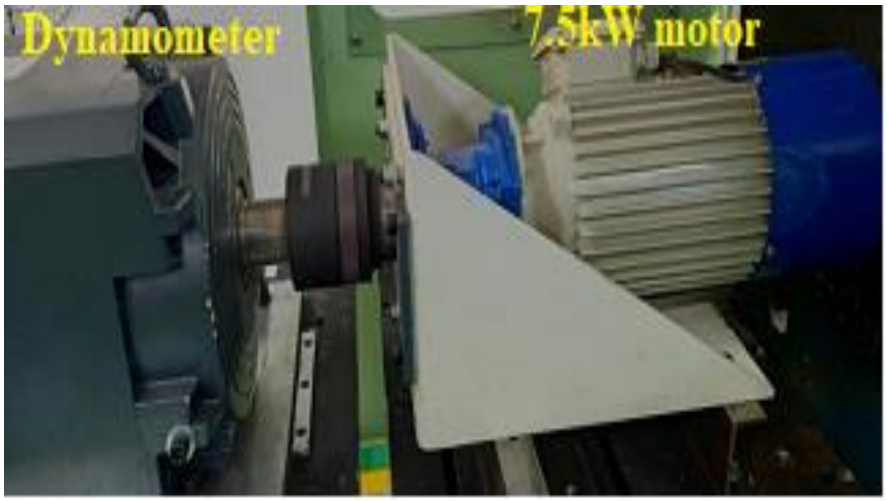

Fig 9: Test setup to load the motor

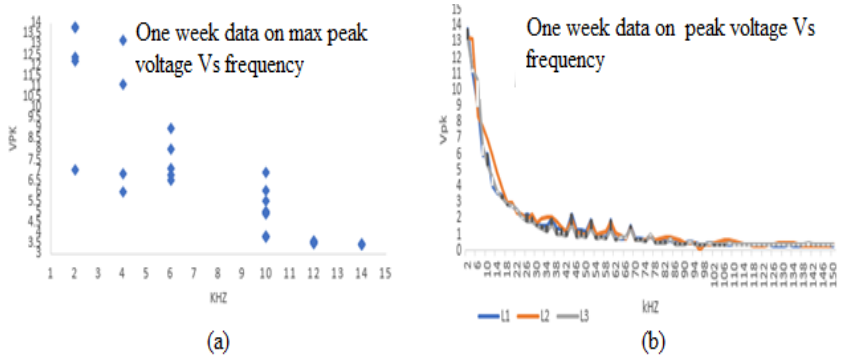

Fig 10: (a) One week data on Supraharmonics maximum peak voltage vs Frequency in kHz. (b) Trend of Phase to Earth graph for three phases 2 kHz to 150 kHz (c) Phase to Earth graph 2 kHz to 150 kHz Conductive emission from PQ meter.

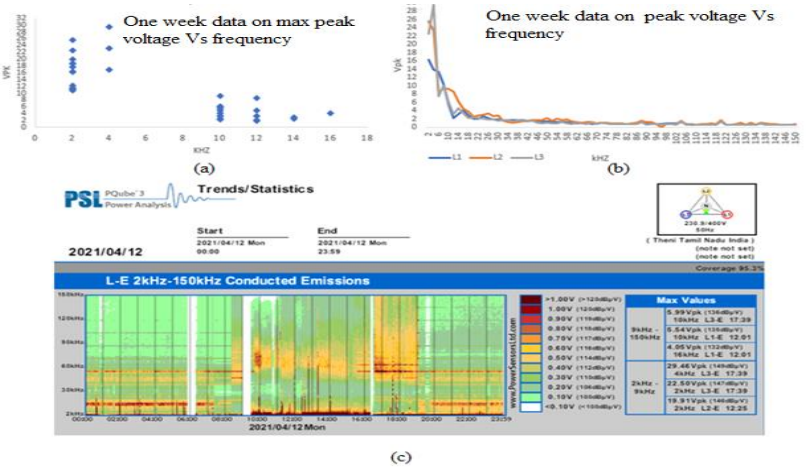

Fig 11: (a) Supraharmonics Peak Voltage vs Frequency (Weekly Data). (b) Phase to Earth Trends (2-150 kHz). (c) Conductive Emission Analysis (2-150 kHz).

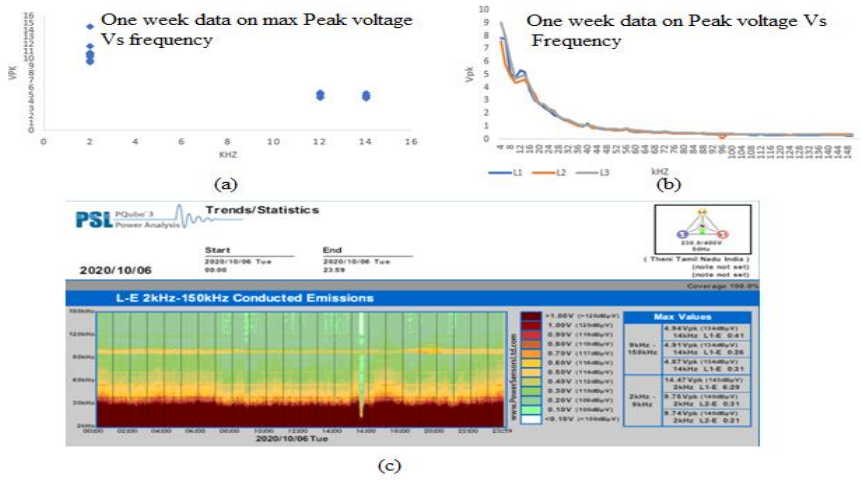

Fig 12: (a) Supraharmonics Observation - Peak Voltage vs Frequency (Weekly). (b) Phase to Earth Trends (2-150 kHz). (c) Conductive Emission Analysis (2-150 kHz).

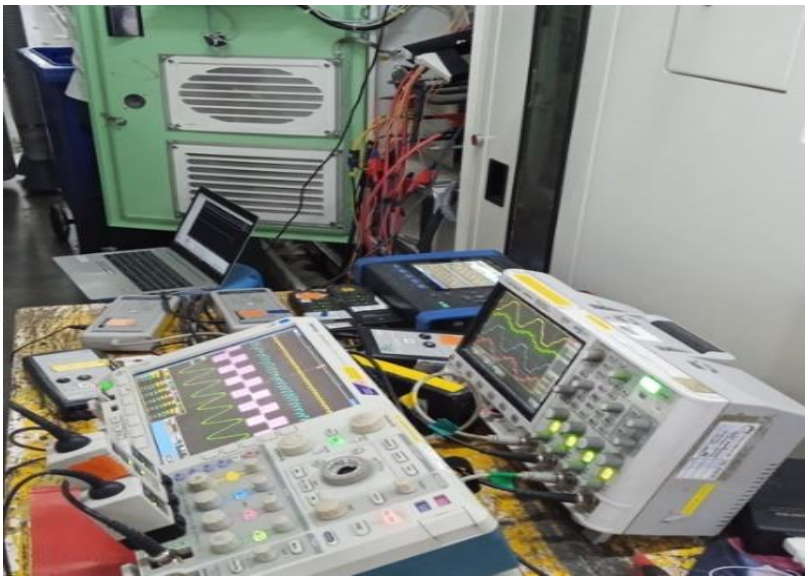

Fig 13: Test set up near to the machine at Site 4

Fig 14: Graph of the actual peak current value captured at Site4.

Fig 15: Comparison of THD

Graph of the actual peak current value captured at Site4 portrays on Fig 14. Comparison of THD is shown on Fig 15.The proposed THD level becomes 0.99%. The existing methods like Random Forest Algorithm (RFA), Cuckoo Search algorithm (CSA) and particle Swarm optimization (PSO)THD becomes 2.5%, 8% and 14%. From this analysis it concludes that the proposed method based THD is less than the existing approaches.

B. Analysis and Real Time Measurement of Supraharmonics

To prove the Supraharmonics presence in Textile mill, five different textile mills are chosen with different geographical location in Tamil Nadu. At site, PSL make PQ tube 3 meter is installed for data capturing. In each site, the data is captured for one week time continuously.

Fig 16 depicts , (a) Phase to Earth graph from 2 kHz to 150 kHz Conductive emission of drive captured from the PQ meter. (b) Trend of Phase to Earth graph for three phases from 2 kHz to 150 kHz, here three phase spectrum is measured and its maximum peak voltage, while observing the data, the high frequency voltage is emitted, and its peak value is captured from the drive in the range of 2.0 kHz to 150 kHz. On observing the graph, the peak voltage emission is observed maximum of 26V. The emission of frequency range is noticed 2 kHz to 10 kHz. Fig 17 illustrates as, (a) Supraharmonics Tracking - Peak Voltage vs Frequency (Weekly). (b) Phase to Earth Trends (2-150 kHz). (c) Conductive Emission Analysis (2-150 kHz). At the time of drive trips and fuse blown, the incoming current reaches to the maximum of 320A, the value is captured through Techtronic's Scope meter.

The Table 1 provides the limits for the disturbance voltage that can be measured at a low voltage alternating current mains power port frequency span of 150 kHz to 30 MHz for apparatus that was measured for Class A and group 1.The CISPR11 standard established two Groups and Classes for the classification of the many kinds of industrial, scientific, and medical apparatus. The Groups are broken down into Group 1 and 2 categories.[8] Apparatus that employed radio frequency energy solely for the internal operation of the apparatus is included in Group 1, which is comprised of all such equipment. Equipment in Group 2 is utilized for the exterior treatment of materials and other procedures of a similar kind. The usage of class A apparatus is permitted throughout all buildings and locations apart from private residences.[9] The machinery classified as Class B is appropriate for use in private households. Within CISPR 11 standard, the restrictions are only stated for the spectrum of 150 kHz to 30 MHz, and the lower spectrum range from 9 kHz to 150 kHz is not included in the specification. Nevertheless, the CISPR11 standard covers the restrictions for home and industrial appliances in the higher spectrum range from 150 kHz to 30 MHz. These limits can be found in the range. The Table 2 provides the limits for the disturbance voltage that can be measured at a low voltage alternating current mains power port in the spectrum span of 150 to 30MHz for apparatus that was measured for Class A and group 2 apparatus. The compatibility values for distortion in voltage at differential mode above 40th harmonic order (exclusive) are presented in the Table 3. The IEC 61000-2-2 discusses about distortion of voltage greater than the 40th harmonic order to 9 kHz and voltage distortion in differential mode between nine to 150 kHz. In differential mode greater than the 40th harmonic order to nine kHz. Voltage distortion over the 40th harmonic order up to 9 kHz is taken into consideration about long-term effects, which is defined as lasting for ten minutes or longer. Voltage distortion at frequencies higher than the 40th harmonic, it is often irrelevant whether the distorted frequencies are at harmonic or inter harmonic frequencies. They can appear at discrete frequencies as well as in rather broad frequency bands. These values are valid up to 9 kHz. These levels apply to frequencies up to 9 kHz. These compatibility levels are related to the voltage distortion levels between any of phase conductors or between any conductor and the neutral conductor, in a bandwidth of 200 Hz.

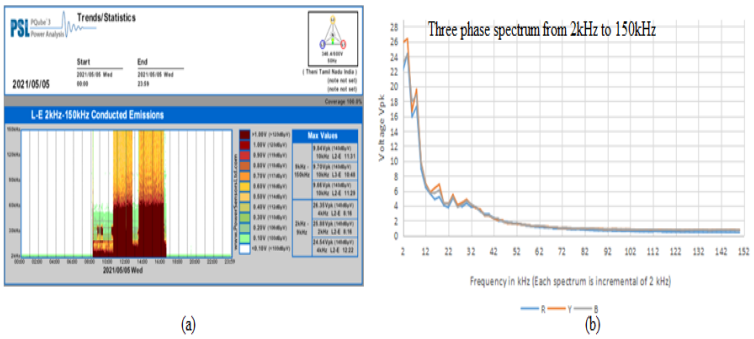

Fig 16: (a) Phase to Earth graph 2 kHz to 150 kHz Conductive emission of drive captured from the PQ meter. (b) Trend of Phase to Earth graph for three phases from 2 kHz to 150 kHz

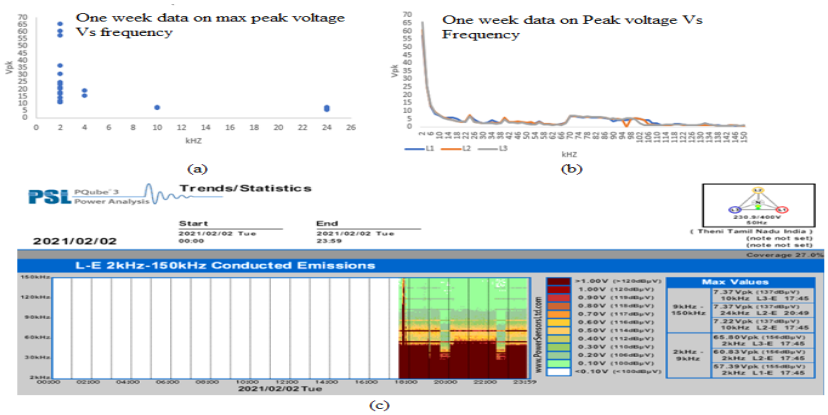

Fig 17: (a) Supraharmonics Tracking - Peak Voltage vs Frequency (Weekly). (b) Phase to Earth Trends (2-150 kHz). (c) Conductive Emission Analysis (2-150 kHz).

Table 1: voltage limits disorder for class A and group 1 apparatus measured on a test site as per CISPR11

Frequency range MHz	**Rated power of $\leq$20 kVA[c]**		**Rated power of >20 kVA and $\leq$75 kVA[a,c]**		**High power electronic systems and equipment, rated power of >75 kVA[b,c]**	
	Quasi-peak $dB(\mu V)$	Average $dB(\mu V)$	Quasi-peak $dB(\mu V)$	Average $dB(\mu V)$	Quasi-peak $dB(\mu V)$	Average $dB(\mu V)$
0.15-0.50	79	66	100	90	130	120
0.50-5	73	60	86	76	125	115
			90	80		
5-30	73	60	Decreasing linearly with logarithm of frequency		115	105
			73	60		

Table 2: voltage limits disorder for class A and group 2 apparatus measured on a test site as per CISPR11.

Frequency range MHz	**Rated power of $\leq$75 kVA[b]**		**Rated power of >75 kVA[a,b]**	
	Quasi-peak $dB(\mu V)$	**Average** $dB(\mu V)$	**Quasi-peak** $dB(\mu V)$	**Average** $dB(\mu V)$
0.15-0.50	100	90	130	120
0.50-5	86	76	125	115
	90	80		
5-30	Decreasing linearly with logarithm of frequency to		115	105
	73	60		

Table 3: Compliance values for distortion in voltage when operating at differential mode on 40th harmonic order 9 kHz as per IEC 61000-2-2

Frequency range kHz	**Compatibility level in %**
2 to 3 for 50 Hz system 2.4 to 3 for 60 Hz system	1.4
3 to 9	1.4 to 0.65

Table 4: Compliance values for distortion in voltage when operating in differential mode above 9 kHz and 150 kHz as per IEC 61000-2-2

Frequency in kHz	**Compatibility level in dB(µV)**
9 to 30	129.5 to 122
30 to 50	122 to 119
50 to 150	113 to 89

Table 5: Motor parameters used for Simulation

Parameter	**Values**
Power	7.5kW
Supply Voltage	400 V
Supply Frequency	50Hz

Rotor Speed	1440 rpm
Stator resistance in ohm	0.6284
Stator inductance in ohm	0.002035
Rotor resistance in ohm	0.6301
Rotor inductance in ohm	0.002045
Mutual inductance in ohm	0.1241

Table 6: Motor and VFD specification at Site 1

Parameter	**Value**
VFD power	55 kW
VFD Intermittent output	135 A
Input voltage of VFD	380-440 VAC
VFD Input current	82 A
Power loss of the VFD	891 W
Motor Power	55 kW
Motor Frequency	87 Hz
Motor Current	110A
Stator poles	4
VFD control algorithm	Voltage vector control

Table 7: Motor and VFD specification at Site 2

Parameter	**Value**
VFD power	7.5 kW
VFD Intermittent output	25.6 A
Input voltage of VFD	380-440 VAC
VFD Input current	14.4 A
Power loss of the VFD	255 W
Motor Power	5.5
Motor Frequency	50
Motor Current	10 A
Stator poles	4
VFD control algorithm	Voltage vector control

Table 8: Motor and VFD specifications at Site 3

Parameter	**Value**
VFD power	75 kW
VFD Intermittent output	159 A
Input voltage of VFD	380-440 VAC
VFD Input current	96 A
Power loss of the VFD	1022 W

Motor Power	75 kW
Motor Frequency	87 Hz
Motor Current	135A
Stator poles	4
VFD control algorithm	Voltage vector control

Table 9: Motor and VFD specifications at Site 4

Parameter	Value
VFD power	75 kW
VFD Intermittent output	159 A
Input voltage of VFD	380-440 VAC
VFD Input current	96 A
Power loss of the VFD	1022 W
Motor Power	75 kW
Motor Frequency	87 Hz
Motor Current	135A
Stator poles	4
VFD control algorithm	Voltage vector control

The compliance limits for distortion in voltage at differential mode between 9 and 150 kHz are presented in the Table 4. Voltage distortion between 9 and 150 kHz is taken into consideration about long-term impacts, which are defined as effects that last for 10 minutes or longer. These compatibility levels are related to disturbance levels measured using a quasi-peak detector and200Hz bandwidth in conformity with CISPR 16-1-1. The limit mentioned Table 3 and 4 reduces linearly with the logarithm of the respective frequency range. Motor parameters used for Simulation is shown in Table 5. At Site 1, the service permitted demand is 3 MVA, where major loads are Ring frame machine. The machines are with nonlinear load with variable frequency drive delivers power to motors. The entire connected load of one machine is 80 kW. Motor and VFD specification at Site 1 are mentioned in Table 6. Motor and VFD specification at Site 2 is shown in Table 7. At Site 2, the service permitted demand is 1 MVA, where the Pqube meter is connected in preparatory machine as the tripping of the variable frequency drive is noticed randomly by the technician. The data is captured for one week continuously. Total load of the machine is 15kW. Motor and VFD specifications at Site 3 is depicted ion Table 8. At Site 3, the service permitted demand is 5 MVA, where the Pqube meter is connected in Ring frame machine. The data is captured for one week continuously. The total load of the machine is 105 kW. Motor and VFD specifications at Site 4 is shown in Table 9. At Site 4, the service permitted demand is 4 MVA, where the Pqube meter is connected in Ring frame machine as the tripping of the variable frequency drive and incoming fuse blown issue is noticed randomly by the technician. The data is captured for one week continuously. The total load of the machine is 105 kW.

VI. CONCLUSION

This study proposes the analysis and measurement of Supraharmonics in a real textile industries based hybrid approaches. As the power electronics device population is high in the industry, maintaining the same in healthy condition is a real challenge to the end users. The proposed method is evaluated in the MATLAB Simulink platform and contrasted with different other existing methods. Many situations including optimal and random scheduling and an elaborate FHO are used to optimizing the switching states of the embedded power converter. The ADKF is used to reduce the dimensionality of data and minimizes the information loss. From the result, it concludes that the proposed approach based reduced the speed compared to existing methods. It is analyses Single Tuned Passive Filter, Textile manufacturing process, supraharmonics. The major objective of the proposed approach is to analysis of Supraharmonics in real textile industries. Analysis of Supraharmonics in a real electrical grid in various textile industry was carried out in and around Tamil Nadu state and it is confirmed

that the presence of Supraharmonics in textile industry causes frequent stoppage of variable frequency drive, early aging of DC choke and incoming fuse blown. The analysis reveals that the magnitude of Supraharmonics and its severity level is high in the Textile industry due to more variable frequency drive is placed for automation and solar power is connected with online grid. The synthesized study data compiled in this research work will be more beneficial to textile equipment manufacturers. The outcomes also demonstrate that the proposed technique performs notably better than the other optimization systems.

Ethical Approval and Consent to participate: This article does not contain any studies with human participants performed by any of the authors.

Human and Animal Ethics: Not Applicable

Consent for publication: Not Applicable

Availability of supporting data: Data sharing does not apply to this article as no new data has been created or analyzed in this study.

Funding: This research did not receive any specific grant from funding agencies in the public,

commercial, or not-for-profit sectors.

Authors' contributions

Y. Dhayaneswaran (Corresponding Author): Conceptualization, Methodology, Writing- Original draft preparation.

A. Amudha: Supervision

Materials and Methods: Not applicable

Results and Discussions: Not applicable

Declarations: Not applicable

Conflicts of interest/Competing interests: Not applicable

Acknowledgements: Not applicable

REFERENCES

[1] T. Yalcin, M. Özdemir, P. Kostyla, Z. Leonowicz. Analysis of supra-harmonics in smart grids. In2017 IEEE International Conference on Environment and Electrical Engineering and 2017 IEEE Industrial and Commercial Power Systems Europe (EEEIC/I&CPS Europe) (pp. 1-4). IEEE. 2017.

[2] J.M. Bentley, P.J. Link. Evaluation of motor power cables for PWM AC drives. InConference Record of 1996 Annual Pulp and Paper Industry Technical Conference (pp. 55-69). IEEE.1996.

[3] Z. Noworolski, P. Eng, U. Reskov. Reducing and utilizing electrical noises for battery monitoring purposes. InINTELEC 2004. 26th Annual International Telecommunications Energy Conference (pp. 611-614). IEEE. 2004.

[4] M. Bollen, M. Olofsson, A. Larsson, S. Rönnberg, M. Lundmark. Standards for supraharmonics (2 to 150 kHz). IEEE Electromagnetic Compatibility Magazine; 3(1):114-9. 2014.

[5] Electromagnetic compatibility (EMC) – Part 2-2: Environment – Compatibility levels for lowfrequencyconducteddisturbances and signalling in public low-voltage power supply systems. IEC 61000-2-2: 2018

[6] Electromagnetic Compatibility (EMC)—Part 4-19: Testing and Measurement Techniques—Test for Immunity to Conducted, Differential Mode Disturbances and Signaling in the Frequency Range 2 kHz to 150 kHz at A.C. Power Ports, Standard IEC 61000-4-19:2014, 2014

[7] J. Yaghoobi, A. Alduraibi, D. Martin, F. Zare, D. Eghbal, R. Memisevic. Impact of high-frequency harmonics (0–9 kHz) generated by grid-connected inverters on distribution transformers. International Journal of Electrical Power & Energy Systems; 122:106177. 2020.

[8] S.K. Rönnberg, A. Gil-De-Castro, R. Medina-Gracia. Supraharmonics in European and North American low-voltage networks. In2018 IEEE International Conference on Environment and Electrical Engineering and 2018 IEEE Industrial and Commercial Power Systems Europe (EEEIC/I&CPS Europe) (pp. 1-6). IEEE. 2018.

[9] Y. Dhayaneswaran, K.V. Murthy, R. Balamurugan. Review on Influence of Electrical Noise on Field Elements. In2011 International Conference on Process Automation, Control and Computing (pp. 1-5). IEEE. 2011.
[10] M. Kaur, S. Kakar, D. Mandal. Electromagnetic interference. In2011 3rd International Conference on Electronics Computer Technology (Vol. 4, pp. 1-5). IEEE. 2011.
[11] G.F. Bartak, A. Abart. EMI in the Frequency Range 2-150 kHz. IEICE Proceedings Series; 18(15P-B1) 2014.
[12] G.L. Skibinski, R.J. Kerkman, D. Schlegel. EMI emissions of modern PWM AC drives. IEEE Industry Applications Magazine; 5(6):47-80 1999.
[13] S.T. Alfalahi, A.A. Alkahtani, A.Q. Al-Shetwi, A.S. Al-Ogaili, A.A. Abbood, M.B. Mansor, Y. Fazea. Supraharmonics in power grid: Identification, standards, and measurement techniques. IEEE Access; 9:103677-90. 2021.
[14] L. Alfieri, A. Bracale, P. Varilone, Z. Leonowicz, P. Kostyla, T. Sikorski, and M. Wasowski, “Methods for assessment of Supraharmonics in power systems.part I: Theoretical issues,” 2019 International Conference on Clean Electrical Power (ICCEP), 2019.
[15] G. Carpinelli, A. Bracale, P. Varilone, T. Sikorski, P. Kostyla, and Z. Leonowicz, “A new advanced method for an accurate assessment of harmonic and SUPRAHARMONIC distortion in power system waveforms,” IEEE Access, vol. 9, pp. 88685–88698, 2021.
[16] Á. Espín-Delgado, S. Rönnberg, S. Sudha Letha, and M. Bollen, “Diagnosis of supraharmonics-related problems based on the effects on electrical equipment,” Electric Power Systems Research, vol. 195, p. 107179, 2021.
[17] L. Alfieri, A. Bracale, P. Varilone, Z. Leonowicz, P. Kostyla, T. Sikorski, and M. Wasowski, “Methods for assessment of Supraharmonics in power systems.part I: Theoretical issues,” 2019 International Conference on Clean Electrical Power (ICCEP), 2019.
[18] O. Sefl and R. Prochazka, “Investigation of supraharmonics' influence on partial discharge activity using an internal cavity sample,” International Journal of Electrical Power & Energy Systems, vol. 134, p. 107440, 2022.
[19] A. Mohos and J. Ladanyi, “Emission measurement of a solar park in the frequency range of 2 to 150 khz,” 2018 International Symposium on Electromagnetic Compatibility (EMC EUROPE), 2018.
[20] M. Morikawa, “Population density and efficiency in energy consumption: An empirical analysis of service establishments,” Energy Economics, vol. 34, no. 5, pp. 1617–1622, 2012.
[21] S. T. Alfalahi, A. A. Alkahtani, A. Q. Al-Shetwi, A. S. Al-Ogaili, A. A. Abbood, M. B. Mansor, and Y. Fazea, “Supraharmonics in power grid: Identification, standards, and measurement techniques,” IEEE Access, vol. 9, pp. 103677–103690, 2021.
[22] G. Carpinelli, A. Bracale, P. Varilone, T. Sikorski, P. Kostyla, and Z. Leonowicz, “A new advanced method for an accurate assessment of harmonic and SUPRAHARMONIC distortion in power system waveforms,” IEEE Access, vol. 9, pp. 88685–88698, 2021.
[23] T. M. Slangen, T. van Wijk, V. Cuk, and J. F. Cobben, “The harmonic and supraharmonic emission of battery electric vehicles in the Netherlands,” 2020 International Conference on Smart Energy Systems and Technologies (SEST), 2020.
[24] Á. Espín-Delgado, S. Rönnberg, S. Sudha Letha, and M. Bollen, “Diagnosis of supraharmonics-related problems based on the effects on electrical equipment,” Electric Power Systems Research, vol. 195, p. 107179, 2021.
[25] D. Y, A. Amudha, and L. Ashokkumar, “Supraharmonics in the electric power grid: Detection and measurement in textile industry,” 2021.
[26] O. Sefl and R. Prochazka, “Investigation of supraharmonics' influence on partial discharge activity using an internal cavity sample,” International Journal of Electrical Power & Energy Systems, vol. 134, p. 107440, 2022.
[27] Z. Hameed, A. Yousaf, W. A. Khan, M. R. Sial, F. Ahmad, and Z. Ghafoor, “Designing of LLCL filter for mitigation of harmonics in smart grid applications and its implementation on Sapphire Textile Industry unit-3,” 2020 International Conference on Emerging Trends in Smart Technologies (ICETST), 2020.
[28] M. T. Riaz, M. M. Afzal, S. M. Aaqib, and H. Ali, “Analysis and evaluating the effect of harmonic distortion levels in industry,” 2021 4th International Conference on Energy Conservation and Efficiency (ICECE), 2021.
[29] M. U. Vivek and P. Selvaprabhu, “Role of telecommunication technologies in microgrids and smart grids,” Smart Grids and Microgrids, pp. 325–364, 2022.

[30] A. N. Skamyin and O. S. Vasilkov, “Power components calculation and their application in presence of high harmonics,” 2019 Electric Power Quality and Supply Reliability Conference (PQ) & 2019 Symposium on Electrical Engineering and Mechatronics (SEEM), 2019.

[31] S. T. Alfalahi, A. A. Alkahtani, A. Q. Al-Shetwi, A. S. Al-Ogaili, A. A. Abbood, M. B. Mansor, and Y. Fazea, “Supraharmonics in power grid: Identification, standards, and measurement techniques,” IEEE Access, vol. 9, pp. 103677–103690, 2021.

[32] C. Palanichamy and N. SundarBabu, “Second stage energy conservation experience with a textile industry,” Energy Policy, vol. 33, no. 5, pp. 603–609, 2005.

[33] H. K. Ozturk, “Energy usage and cost in textile industry: A case study for Turkey,” Energy, vol. 30, no. 13, pp. 2424–2446, 2005.

[34] D. Shen, “What's happening in China's textile and clothing industries?,” Clothing and Textiles Research Journal, vol. 26, no. 3, pp. 203–222, 2008.

[35] O. Todorov, O. Bialobrzheskyi, and S. Andrii, “Application of IEEE 1459-2010 for the power investigation a traction substation transformer secondary voltage,” 2020 IEEE KhPI Week on Advanced Technology (KhPIWeek), 2020.

[36] C. Gopalakrishnan, K. Udayakumar, and T. A. Raghavendiran, “Survey of harmonic distortion from power quality measurements and the application of standards including simulation,” IEEE/PES Transmission and Distribution Conference and Exhibition.

[37] Y. K. Sharma and M. R. Vijay, “Capacitor banks and its effect on power system with high harmonics loads,” 2018 3rd International Conference for Convergence in Technology (I2CT), 2018.

[38] D. Mukherjee, P. Das, and S. Banerjee, “Comparative analysis of different filters in power line harmonic reduction,” 2015 International Conference on Applied and Theoretical Computing and Communication Technology (iCATccT), 2015.

[39] T. Halder, “Harmonic analysis of the trapezoidal waves in the power quality issues,” 2020 IEEE 17th India Council International Conference (INDICON), 2020.

[40] G. Anu and F. M. Fernandez, “Identification of harmonic injection and distortion power at customer location,” 2020 19th International Conference on Harmonics and Quality of Power (ICHQP), 2020.

[41] M. Ahmed, N.-A.-Masood, and T. Aziz, “An approach of incorporating harmonic mitigation units in an industrial distribution network with renewable penetration,” Energy Reports, vol. 7, pp. 6273–6291, 2021.

[42] A. Alizade and J. B. Noshahr, “Evaluating noise and DC offset due to inter-harmonics and supra-harmonics caused by back-to-back converter of (DFIG) in AC Distribution Network,” CIRED - Open Access Proceedings Journal, vol. 2017, no. 1, pp. 629–632, 2017.

[43] L. Alfieri, A. Bracale, G. Carpinelli, and A. Larsson, “A wavelet-modified esprit hybrid method for assessment of spectral components from 0 to 150 KHz,” Energies, vol. 10, no. 1, p. 97, 2017.

[44] T. Busatto, A. Larsson, S. K. Rönnberg, and M. H. J. Bollen, “Supraharmonics emission assessment of multi-level converters applied for photovoltaic grid-connected inverters,” Renewable Energy and Power Quality Journal, vol. 1, no. 15, pp. 143–148, 2017.

[45] J. G. V. Montoya, E. G. Luna, and E. M. Sáenz, "Power Quality Assessment of the Interconnection of a Microgrid to a local distribution system using Real-Time Simulation," Ph.D. dissertation, Universidad Nacional de Colombia, DYNA, pp. 28-33, 2020.

[46] P. Kishore and D. N. Kumar, "Performance and Comparison of Harmonics Using Active Power Filters and DVR in Low-Voltage Distributed Networks," in Innovations in Electrical and Electronics Engineering, 2nd ed., Western Electric Co., Springer 2020.

[47]] L. E. Christian, L. M. Putranto, and S. P. Hadi, "Design of Microgrid with Distribution Static Synchronous Compensator (D-STATCOM) for Regulating the Voltage Fluctuation," presented at IEEE 7th International Conference on Smart Energy Grid Engineering (SEGE), 2019.

[48] J.-ho Ahn, J.-C. Yoon, and I.-K. Lee, “Depth-based anisotropic Kuwaharafiltering,” ACM SIGGRAPH 2010 Posters, 2010.

[49] M. P. Kumar, B. Poornima, H. S. Nagendraswamy, and C. Manjunath, “Structure-preserving NPR framework for Image Abstraction and stylization,” The Journal of Supercomputing, vol. 77, no. 8, pp. 8445–8513, 2021.

[50] M. Azizi, S. Talatahari, and A. H. Gandomi, “Fire hawk optimizer: A novel Metaheuristic algorithm,” Artificial Intelligence Review, vol. 56, no. 1, pp. 287–363, 2022.